Numerical Investigation of HSC Columns Retrofitted by CFRP Materials under Combined Load

Mohammed El Youbi [1*], Taoufik Tbatou [2], Imad Kadiri [1], Saïf Ed-Dîn Fertahi [3]

[1] *Laboratoire d'Etude des Matériaux Avancés et Applications, EST de Meknes, Université Moulay Ismail (UMI), Meknès, Morocco.*

[2] *LSIB Laboratory, FST Mohammedia, Hassan II University of Casablanca, Morocco.*

[3] *Energy Research Center, Physics Department, Faculty of Science, Mohammed V University in Rabat, Rabat 1014, Morocco.*

Abstract

Repairing and retrofitting old civil engineering structures based on reinforced concrete represents a challenge for civil engineering societies all over the world. Environmental impacts such as corrosion and natural disasters like earthquakes can considerably weaken those structures. Reinforced concrete confinement technique using carbon fiber-reinforced polymers (CFRP) is considered as an innovative solution to strengthen the old and damaged structures. In this paper, a numerical simulation was carried out to evaluate the impact of the CFRP jacket as a confining composite material on the compressive strength and the ultimate strain of confined reinforced concrete. A FE model was developed, validated by comparing its results with the available experimental measurements, and finally assessed by performing a parametric study. Indeed, the parametric investigations had as their purpose the evaluation of the level of confinement (different number of plies), namely without plies, one plie, and three plies configuration, that were subjected to different eccentric loading modes e=0, e=25 and e=50 mm, in order to assess the interaction between the combined load that can be represented by compressive and flexural effect. The numerical results were, in fact, in good agreement with the experimental data. In addition, CFRP wrapping had a significant effect on the maximum load of eccentrically loaded columns compared to concentrically loaded columns by increasing the compressive strength with a value of 15% gain compared to the unconfined column.

Keywords: Composite Materials; Civil Engineering; Structures; Reinforced Concrete; FEA.

1. Introduction

In civil engineering, several high-strength concrete HSC structures were built according to old design codes before the implementation of the new seismic design guidelines [1-3]. These structures contain non-ductile reinforced concrete columns, which can suffer extensive damage when subjected to an earthquake. The failure of these columns is mainly due to the lack of shear resistance ability and insufficient ductility provided by a small amount of transverse steel. The ductility of a reinforced concrete column plays a very important role in failure prevention. This is why many research works in the last two decades try to improve the ductility of reinforced concrete columns and therefore the safety of the structures [4-7]. One of the effective ways to improve the ductility of a column is by repairing damaged reinforced concrete members by the external bonding of fiber reinforced polymer (FRP) laminates [8]. Moreover, strengthening of old RC structures is more economical than demolition and reconstruction. The use of FRP composites with an elongation

greater than 5% [9, 10] is a very effective solution for seismic strengthening of RC structures. Many other benefits are offered by the use of FRP, such as excellent strength to self-weight ratio, high tensile strength, large fatigue resistance capacity, and high durability [4, 11]. That is why the mechanical behavior of the strengthening techniques should be understood to make the best decision for rehabilitation and to save time and cost.

Various reinforcement techniques for reinforced concrete structures are presented by Fukuyama & Sugano (2000), Wu & Eamon (2017) and Beroual & Samai (2021) [12-14]. Among those techniques, the classical approaches consist of:

- Reinforcement by adding new elements such as bracing, walls, infill...etc.

- The use of components linking the elements added to the old ones.

- Reinforced concrete columns lining with traditional materials such as steel or reinforced concrete in order to improve bending and shear performance.

- Containment of column-beam junctions with steel elements.

In the last two decades, reinforced concrete confinement technique using fiber-reinforced polymer (FRP) fabrics has experienced significant growth. These new-generation materials offer high mechanical performance / weight ratio, high resistance to corrosive environments, as well as great ease of use and implementation.

Several numerical and experimental studies have been conducted on the reinforcement of concrete columns using composite materials. In fact, concrete columns are subjects to degradation factors such as steel corrosion and alkali-silica reaction and exceptional loads such as earthquakes and explosions. In order to overcome the consequences of those constraints, like lap-splice, shear and flexural deficiency [15], civil engineering researchers over the world have proposed columns confinement using materials with high resistance to aggressive environmental factors. Among those materials, Fiber-Reinforced Polymers (FRP) has had a high interest in the last decade. In fact, de Diego et al. (2019) [16] have recently conducted a study in order to estimate the FRP jacket ultimate strain, which is mandatory in the evaluation process of the confined concrete strength. Indeed, the authors have carried out an experimental program on 38 square sections of confined concrete using FRP. Results have shown that the ductility and strength of the concrete columns can be increased considerably using FRP confinement. In addition, a correlation has been established between the corner radius and the ultimate strain, which should be taken into account in the case of non-circular sections.

In the same context, Fanaradelli et al. (2019) [17] conducted a study on the impact of FRP confinement on stress and strain at the failure of square and rectangular section concrete columns. This study consists of a database evaluation of several models in order to predict the peak and the ultimate conditions. Hasan et al. (2019) [18] have proposed a novel equation for the numerical calculations of the axial peak load. This study has shown that the use of FRP bars elasticity modulus is more accurate than the ultimate tensile strength for longitudinal FRP bars. Abdulla & Khaduier (2018) [19] have carried out a numerical study using ANSYS in order to investigate the impact of Carbon FRP (CFRP) composites on strength and ductility. They have studied the effect of the major parameters which influence the contact between the CFRP and the concrete column. Among those major parameters, compressive strength of concrete, corner radius of square columns and elasticity modulus have been calculated. The results of this study have shown that the numerical analysis using ANSYS is in good line with the experimental results.

Al-Rousan (2020) [20] has also conducted a numerical simulation to quantify the impact of CFRP confinement on circular reinforced concrete columns. In this Finite Element Analysis (FEA), the author has used respectively SOLID65, SOLID45, LINK8 and SOLID46 as elements representing concrete, steel plates, discrete reinforcing steel bars and CFRP sheets. Results of this numerical study have shown that the number of CFRP sheet layers can significantly impact the ultimate axial strength and the ultimate displacement of the circular columns. Hawileh et al. [21] have developed a new Finite Element (FE) model with the aim of testing and verifying the influence of critical parameters on the externally side bonded FRP systems. The validation process was carried out using experimental data. Results have shown that the side-bonding FRP systems represent a good alternative to increase the flexural capacity of reinforced concrete beams.

Al-Nimry & Neqresh (2019) [22] have conducted an experimental study to investigate the axial flexural interaction of CFRP-jacketed RC columns with the aim of testing the impact of CFRP on the axial and bending capacities of the wrapped columns. Hence, 23 square column samples with one-third scale were tested using several eccentric axial compression loads (0, 35, 50 and 65 mm). A comparison has been carried out between the unwrapped RC columns and the wrapped with one and two plies of CFRP. Results have shown that the fibers orientations have a considerable effect on axial resistance. Indeed, the use of CFRP hoop confining system has increased the axial resistance in the case of eccentrically loaded RC columns. In addition, the combination between axially-oriented CFRP sheets and the hoop confining system has increased the axial resistance of the RC columns by around 18%. Nevertheless, this combination has slightly decreased the ductility and toughness of the tested columns compared with the control specimens. In the same context, Mhanna et al. (2019) [23] have conducted an experimental study to compare the effectiveness and the impact of two CFRP wrapping configurations on externally bonded RC beams. The two studied configurations are the U-Wrapped T-beam and the completely wrapped rectangular beam. The results of those experimental tests have shown

that the U-Wrapped scheme has increased the shear strength of the T-beam by 114.82% compared by the control T-beam. In terms of ductility, the completely wrapped scheme has shown better results than those of the U-Wrapped T-beam specimen. The experimental works, as well as the traditional numerical and/or analytical models are unable to reproduce precisely the behavior complexity of reinforced concrete-based structures. In fact, these models can be hardly used in an approach of design and calculation for structural reinforcement.

The literature review presented in the previous sections shows that the existing experimental and numerical model on the effectiveness of FRP jacketing in HSC columns under combined loads (axial loading and bending moment) is still limited. In this paper, the authors aimed at providing better understanding of the stress-strain relationship of confined HSC columns. Both unconfined and CFRP-confined columns were established under different solicitations covering a wide series of axial loading eccentricities. Therefore, a set of numerical models of HSC confined columns were created and developed by varying the main jacket parameters selected from previous research study [24, 25], the obtained results were tested and validated with experimental and numerical results available on the literature. The proposed FE model is shown to be accurate and perform better than the existing numerical models of the same type in predicting existing test results.

2. Materials and Methods

2.1. Description of the Case Study

The experimental investigation of Hadi et al. [24] was applied to verify the developed FE model for strengthening RC column retrofitted by CFRP using an FEM code [25]. The column model was subjected to an axial compressive loading on their top face, while the bottom side was restrained. The column models had a typical cross section of 200 mm×200 mm with the height of 800 mm as listed in Table 1. The concrete cover was 20 mm on each side of the specimen and at the top and bottom as well. A corner radius of 34 mm was applied to the specimens. The specimens have four N12 (12 mm diameter deformed bars) as longitudinal steel reinforcement and R8 (8 mm diameter plain bars) spaced at 100 mm as transverse steel reinforcement (ties). The R8 ties spaced at 50 mm were applied at both ends of the specimens to prevent premature failure at the locations. Figure 1 shows the details of the reinforcement.

Table 1. Configuration of the tested specimens

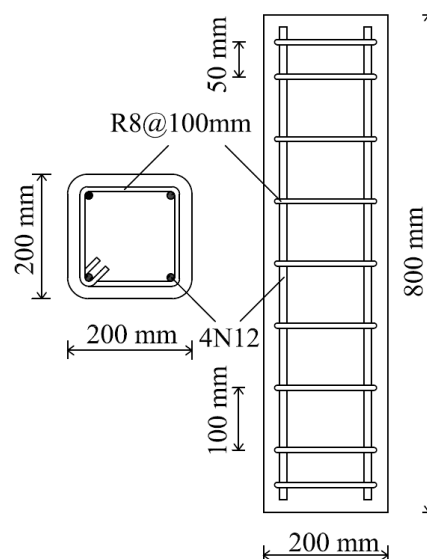| Test specimen	Side Width (mm)	Height (mm)	Internal Reinforcement	Number of FRP Layers	Eccentricity (mm)
0C0					0
0C25	200	800	4N12 and R8 @ 100 mm	None	25
0C50					50
1HC0					0
1HC25	200	800	4N12 and R8 @ 100 mm	1 Layer	25
1HC50					50
3HC0					0
3HC25	200	800	4N12 and R8 @ 100 mm	3 Layers	25
3HC50					50

Figure 1. Geometric details of the tested and modeled RC column specimens

The control column was externally strengthened by bonding layers of CFRP fabric with 0.45 mm thickness tilted at an angle of 0° to the transversal axis of the column. The tensile strength, tensile strain, and elastic modulus of the CFRP were 1399 MPa, 1.86% and 75.4 GPa, respectively. The first column specimen was made from reinforced concrete under concentric loading, namely specimen 0C0. The eight remaining column specimens had various number of plies and different cases of eccentricity loading (as shown in Table 1). The mechanical properties of each used specimen for the validation analysis were adopted in the development of the numerical models in order to predict with accuracy the behavior of each column specimen.

2.2. Material Properties

2.2.1. HSC Concrete

The development of high-strength concrete HSC has considerably progressed with the increase of construction of high-rise buildings. The HSC has been defined as concrete with a cylinder compressive strength exceeding 50 MP. It was developed and applied to columns under high level axial forces, such as columns of lower floors in high-rise buildings, bridges, and offshore structures. The mechanical and the durable properties of HSC were the basis for the various applications. In this study, the concrete presents a high compressive strength of 79.5 MPa. Figure 2-a shows a typical stress-strain curve for concrete material [25]. The concrete is modeled using SOLID65 ANSYS element type to model the HSC columns specimens. This element can capture both tension cracks and compression crushing. It has eight nodes with three degrees of freedom at each node. A schematic representation of the element is shown in Figure 2-b.
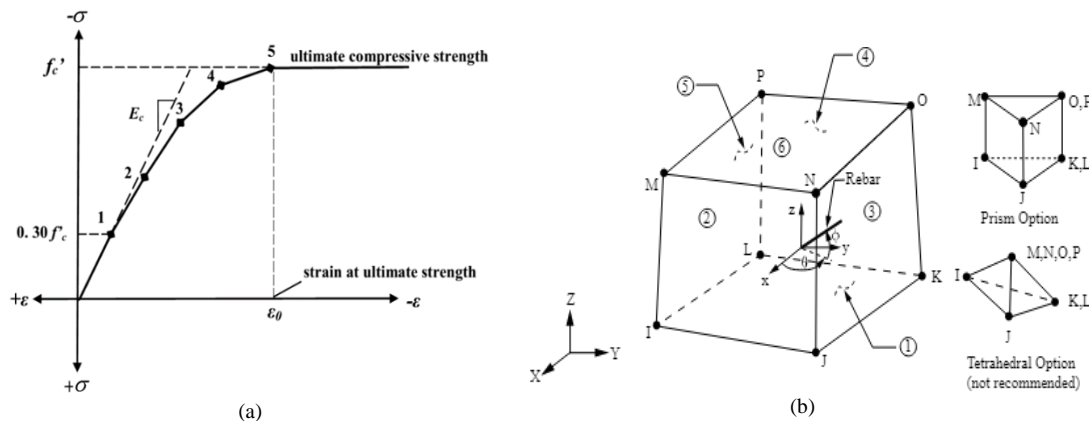

Figure 2. (a) Uniaxial stress-strain behavior of concrete; (b) SOLID65 ANSYS element [25]

The nonlinear behavior of concrete under compression were assigned to the developed numerical models throughout defining the uniaxial stress-strain relationship, obtained by using modified Hognestad piecewise model [26]. The equations (Equations 1 to 4) are used to calculate the stress-strain relationship curve for the HSC concrete.

$$E_c = 5000\sqrt{f_{ck}} \tag{1}$$

$$f = \frac{E_c \varepsilon}{1 + \left(\dfrac{\varepsilon}{\varepsilon_0}\right)^2} \tag{2}$$

$$\varepsilon_0 = \frac{2 f_{ck}}{E_c} \tag{3}$$

$$E_c = \frac{f}{\varepsilon} \tag{4}$$

2.2.2. Steel Reinforcement

The tensile strength tests were conducted on the reinforcing steel bars to determine their tensile strength. Average tensile yield strengths of 564 and 516 MPa were obtained for N12 and R8 reinforcing bars, respectively. The steel for the FE model is supposed to be an elastic-perfectly plastic material and bilinear under monotonic tension and compression (Figure 3-a). The LINK 180 ANSYS element is used to model longitudinal and transversal reinforcements bars. The geometry and node locations for this element type are shown in Figure 3-b.
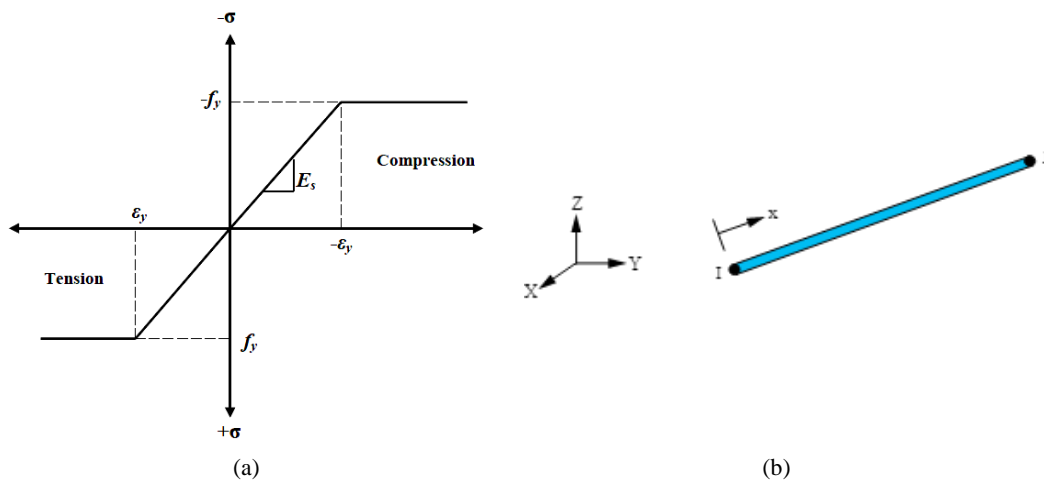
Figure 3. (a) Stress-strain curve for the steel reinforcement; (b) LINK 180 ANSYS element

2.3. Setting Equations of the FRP-Confined Concrete in Rectangular Columns

Due to the non-uniformity of confinement, the axial stress of concrete in an FRP-confined rectangular column varies over the section. Thus, to develop the stress–strain models, the average axial stress is used. Lam & Teng and Teng et al. (2003) [27, 28] presented a stress–strain model for FRP-confined concrete in rectangular columns, which was modified from their earlier model for concrete uniformly confined by FRP [27, 28]. A rectangular column with rounded corners is presented in Figure 4. Square columns are considered as a special case of rectangular columns with b=h. The aspect ratio h/b defines the shape of a rectangular section. To improve the effectiveness of FRP confinement, corner rounding is generally recommended. Due to the presence of internal steel reinforcement, the corner radius r_c is generally limited to small values.
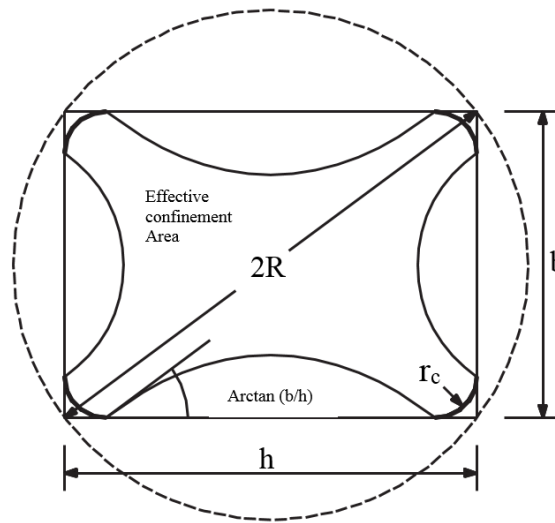

Figure 4. Lam & Teng and Teng et al. (2003) [27, 28] model for FRP-confined concrete in rectangular sections

In rectangular RC columns, the shape of the stress–strain curve is described in Lam & Teng (2003) [27], but the ultimate point is redefined by introducing two shape factors and the concept of an equivalent circular column. The compressive strength is presented in Equations 5 and 6, which takes into account a shape factor denoted by k_{s1}.

$$\frac{f'_{cc}}{f'_{co}} = 1 + 3.3 k_{s1} \frac{f_l}{f'_{co}}, \quad k_{s1} \frac{f_l}{f'_{co}} \geq 0.07 \tag{5}$$

$$\frac{f'_{cc}}{f'_{co}} = 1, \quad k_{s1} \frac{f_l}{f'_{co}} \langle 0.07 \tag{6}$$

where the term $k_{s1} \frac{f_l}{f_{co}}$ is the effective confinement ratio. Similarly, the ultimate axial strain is given by the Equation 7 in which a different shape factor, k_{s2}, is introduced:

$$\frac{\varepsilon_{cu}}{\varepsilon_{co}} = 1.75 + 12 k_{s2} \frac{f_l}{f'_{co}} \left(\frac{\varepsilon_{h,rup}}{\varepsilon_{co}} \right)^{0.45} \tag{7}$$

In Equations. 5, 6 and 7, f_l is the confining pressure in an equivalent circular column. The equivalent circular column has a radius R , presented in Equation 8, being equal to half the diagonal distance of the section.

$$R = \frac{1}{2}\sqrt{h^2 + b^2} \tag{8}$$

It is commonly accepted that for non-circular columns, the confinement efficiency of CFRP is much less effective than the circular columns due to the presence of sharp corners and non-uniform confinement loads in Lam & Teng and Teng et al. (2003) [27, 28] model. The effective confinement zone is contained by four parabolas as illustrated in Figure 4. The effective confinement area ratio $\frac{A_e}{A_c}$ is therefore expressed by Equation 9:

$$\frac{A_e}{A_c} = \frac{1 - \left[\dfrac{\dfrac{b}{h}(h - 2r_c)^2 + \dfrac{h}{b}(b - 2r_c)^2}{3A_g}\right] - \rho_c}{1 - \rho_c} \tag{9}$$

where A_e and A_c are the effective confinement zone and the total cross-sectional zone of concrete confined by the FRP laminate, A_g is the gross zone section with rounded corners and ρ_c is the cross-sectional zone ratio of the main steel reinforcement.

The two shape factors, one for strength enhancement k_{s1} and the other for strain enhancement k_{s2}, are then expressed by Equations 10 and 11:

$$k_{s1} = \left(\frac{b}{h}\right)^2 \frac{A_e}{A_c} \tag{10}$$

$$k_{s2} = \left(\frac{b}{h}\right)^{0.5} \frac{A_e}{A_c} \tag{11}$$

2.4. Boundary Conditions and Meshing

In order to avoid convergence problems that were encountered in the FEM software [25], owing to singularities in the tangent stiffness arising from the softening material model, the load was applied in several sub-steps in such a way that it gradually increases at a constant rate from zero to a predefined final load. An identical mesh size was adopted for the concrete, steel and FRP elements. This mesh size was sufficient to ensure the independence mesh study. Figure 5-a shows the FEM model and the meshing elements of steel and CFRP, while Figure 5-b illustrates the mesh of the column, the boundary conditions and the applied displacement. A flowchart of the procedures is presented in Figure 6.
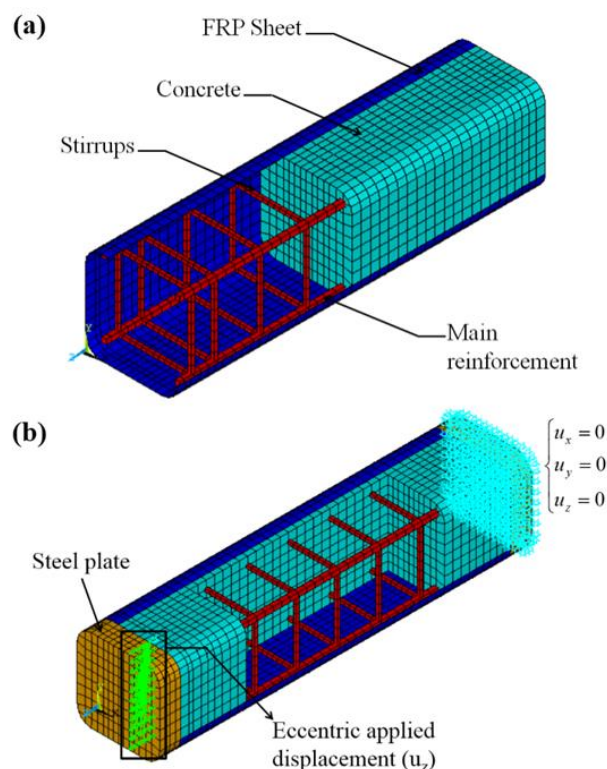

Figure 5. (a) Finite element components for column with CFRP laminate; (b) Assigned boundary conditions
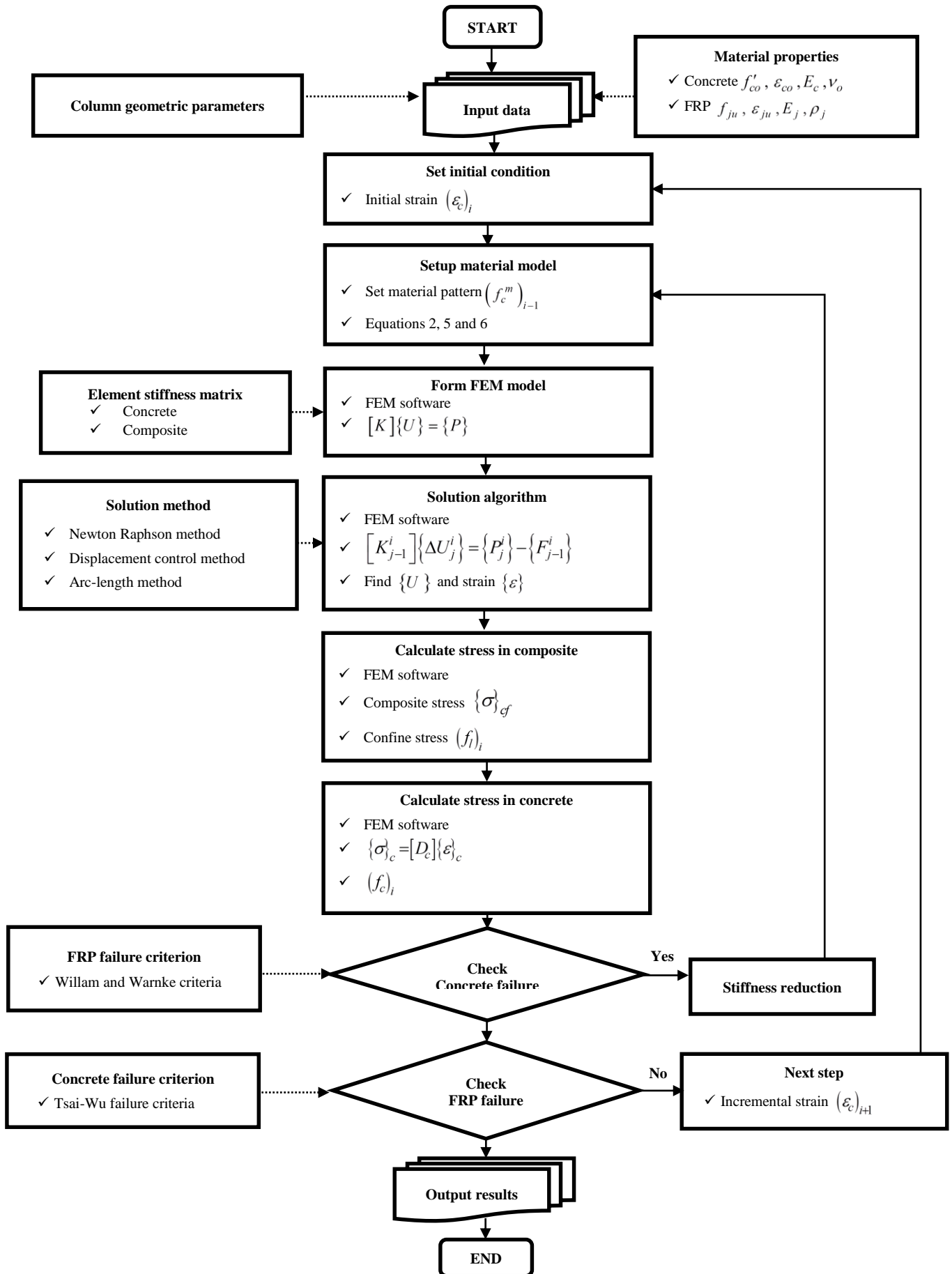
Figure 6. Flowchart of the non-linear program

3. Results and Discussion

In this section, the performance of the proposed column model, which is a square section specimens confined with a CFRP composite is investigated through numerical simulations using an FEM code [25]. The experimental tests which serve as a reference for this analysis were based on the work of Hadi & Widiarsa (2012) [24] that were, in fact, evaluated using a numerical approach by Abdulla & Khaduier (2018) [19], in order to validate numerically the nonlinear mechanical behavior of the concrete.

The accuracy of the numerical results is assessed with respect to its capacity to predict the ultimate resistance (f_{cc}) and the ultimate axial displacement (U_z) of the specimens confined by CFRP jacket. The numerical results are presented for the different specimens that were proposed in the parametric study as shown in Tables 2 and 3, which summarizes respectively the predictions of these quantities (f_{cc}) and (U_z) besides to the relative errors between the obtained numerical results and the available experimental and numerical data.

Table 2. Experimental and numerical results of the ultimate load

			Ultimate load (kN)			
Columns	EXP [24]	FEM [19]	Our Num. results	Error (%) Exp./FEM	Error (%) Exp./ Our Num. results	Error (%) Our Num. results/FEM
0C0	3248	3185	3249	1.94	0.03	1.97
0C25	1950	1786	1832	8.41	6.05	2.51
0C50	1336	1268	1277	5.09	4.42	0.70
1HC0	3279	3174	3489	3.20	6.40	9.03
1HC25	2076	1986	2145	4.34	3.32	7.41
1HC50	1433	1512	1514	5.51	5.65	0.13
3HC0	3585	3369	3684	6.03	2.76	8.55
3HC25	2269	2091	2234	7.84	1.54	6.4
3HC50	1534	1467	1599	4.37	4.24	8.25

Table 3. Experimental and numerical results of the axial displacement

			Axial Displacement (mm)			
Columns	EXP [24]	FEM [19]	Our Num. results	Error (%) Exp./FEM	Error (%) Exp./Our Num. results	Error (%) Our Num. results/FEM
0C0	4.58	4.57	4.42	3.49	0.09	3.53
0C25	3.91	4.26	4.05	3.58	8.39	5.38
0C50	3.86	4.07	3.89	0.78	5.37	4.86
1HC0	4.53	4.55	4.45	6.18	0.64	2.45
1HC25	4.45	4.68	4.63	4.04	5.08	1.25
1HC50	4.05	4.28	4.26	5.19	5.40	0.49
3HC0	5.29	5.83	5.85	10.59	9.31	0.29
3HC25	4.48	4.45	4.61	2.90	0.52	3.32
3HC50	3.99	4.00	4.1	2.76	0.35	2.34

The investigations were carried out on the unconfined test specimens with three different eccentricities e=0, e=25 and e=50 mm (0C0, 0C25 and 0C50). The effect of eccentricity on the behavior of columns can be seen in Figure 7. It can be clearly seen that the eccentricity of the applied loads reduced the load carrying capacity and performance of the columns.
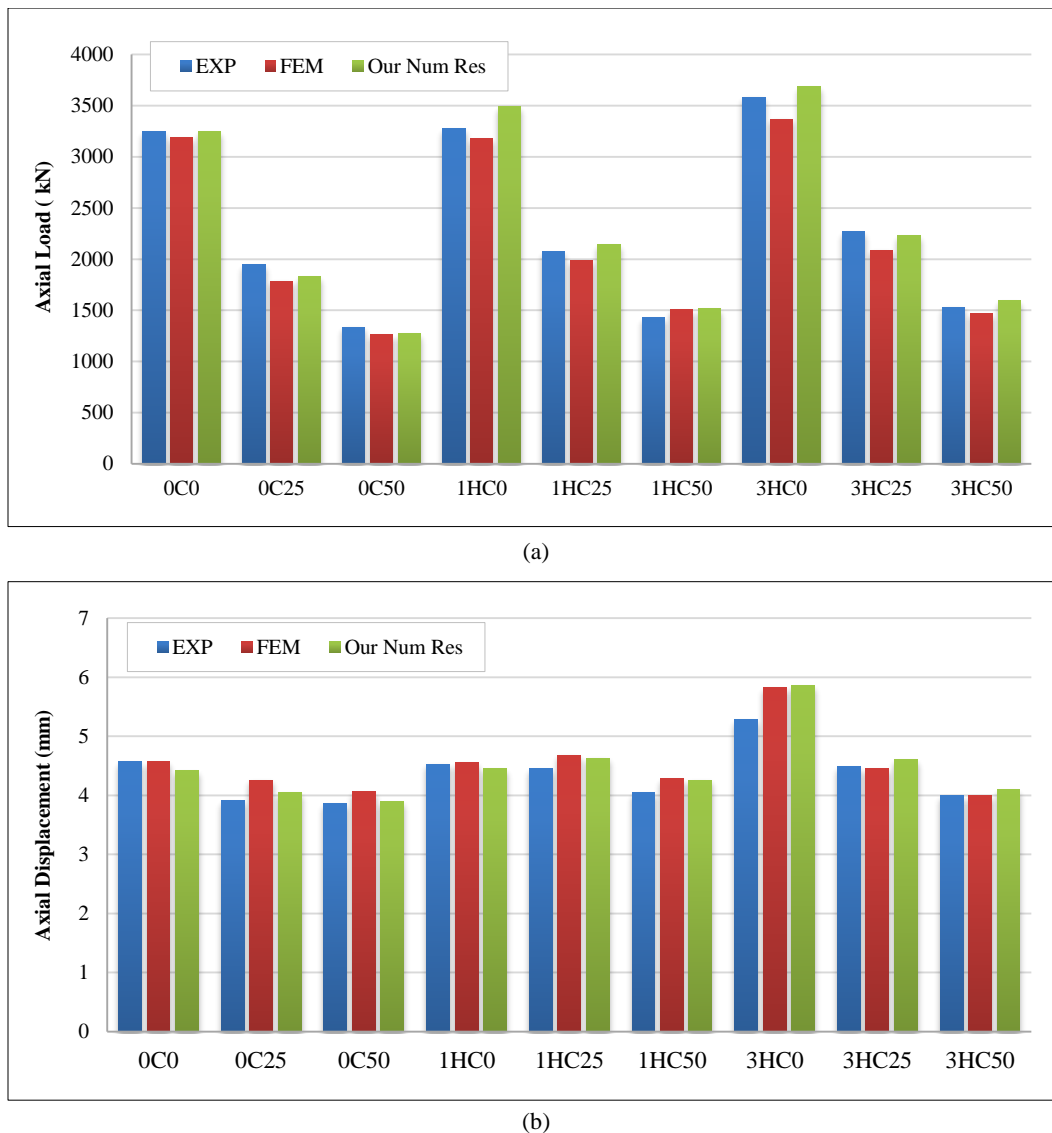
(a)

(b)

Figure 7. Effects of loading eccentricity on (a) axial load resistance; (b) axial displacement

The load-carrying capacity of the unconfined CFRP columns decreased by about 44 and 60 % under 25- and 50-mm eccentricities, if compared to unwrapped concentric CFRP columns, respectively (0C25 and 0C50). Considering the confined specimens (1HC25 and 1HC50), the average strength drops were 38 and 57% for one-layer columns tested with 25- and 50-mm eccentricity, respectively. On the contrary, the average strength drops were 39 and 57% for (3HC25 and 3HC50), if compared with three-layer columns tested with zero eccentricity (3HC0). The decrease of the load-carrying capacity with the increase of the eccentricity can be explained by the increase of eccentricity, the stress gradient over the column cross section increases to a nonuniform confining load and hence a decrease of column load carrying capacity.

It can be seen that the specimen (1HC0, 1HC25 and 1HC50) with one layer of CFRP did not improve significantly the load carrying capacity and performance of the column under combined load. However, the specimens (3HC0, 3HC25 and 3HC50) with three layers of CFRP showed a large improvement in its load carrying capacity compared to the other cases.

The axial load versus axial displacement curves of modelled columns were shown in Figure 8, that compares different confinement levels (0C0, 1C0 and 3C0) obtained by FRP composites based on carbon fibers for the same concrete of high compressive strength of f_c=50MPa. It can be seen that the (3C0) specimens' columns showed a higher gain in the ultimate axial displacement (33 %) more than the gain in strength compared to (0C0 and 1C0) specimens. Therefore, the resistance (load-carrying capacity) and the ductility (deformation capacity) of the tested columns confined with CFRP were improved significantly.
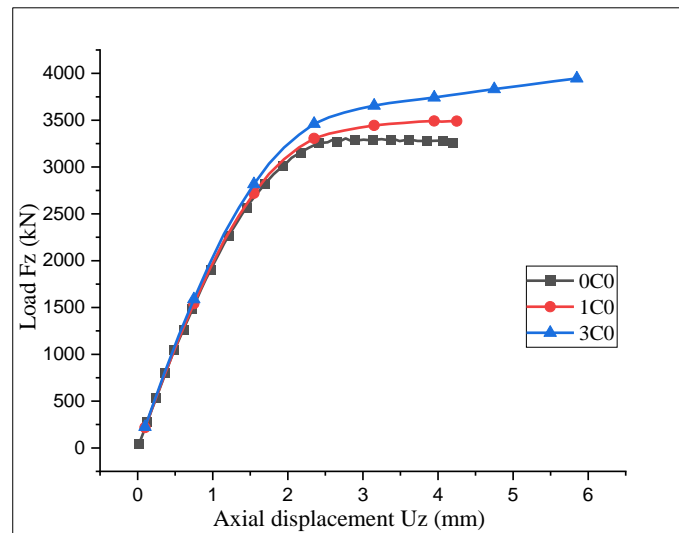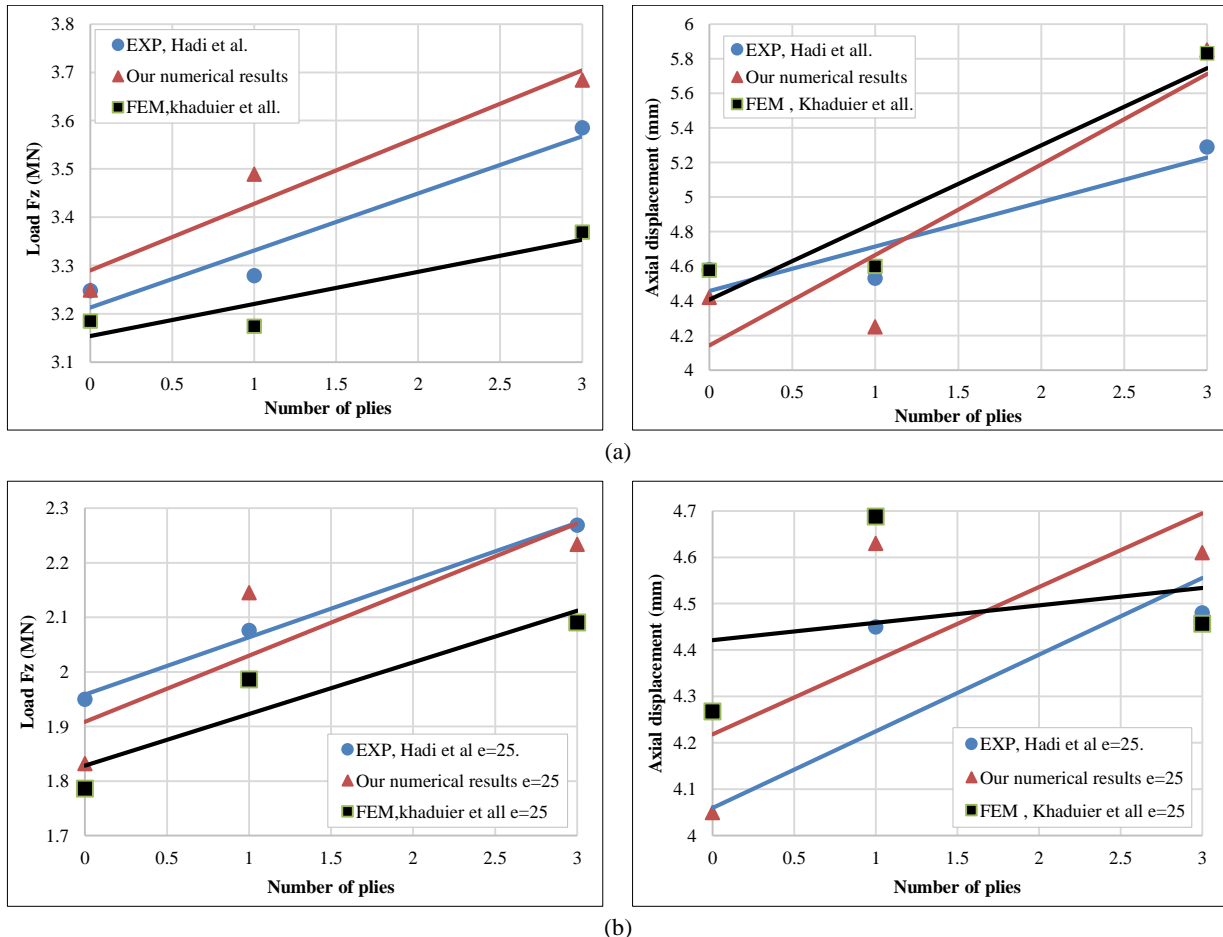
Figure 8. Load displacement curves for columns under concentric loading (numerical results)

The quality of the confinement depends on the mechanical characteristics of CFRP besides the number of plies used in the lining of the specimens. For (0C0) specimens, the load-displacement curves show a slope which follows that of the unconfined concrete up to the point of inflection.

The effect of confinement level on the enhancement in peak load and axial displacement is illustrated in Figure 9. The confinement considerably increases the ultimate loads and the axial displacements of the 3C0 specimens with three layers of CFRP, which presents a gain in resistance with compression and axial displacement respectively of 10.4% and 15.5%. However, for the specimens confined with 1-layer 1C0, the gains in resistance and strain are less pronounced than previously (less than 2%). It should be noted that CFRP wrapping had a more significant effect on the maximum load of eccentrically loaded columns compared to concentrically load columns by increasing the compressive strength with a value of 15% of gain.
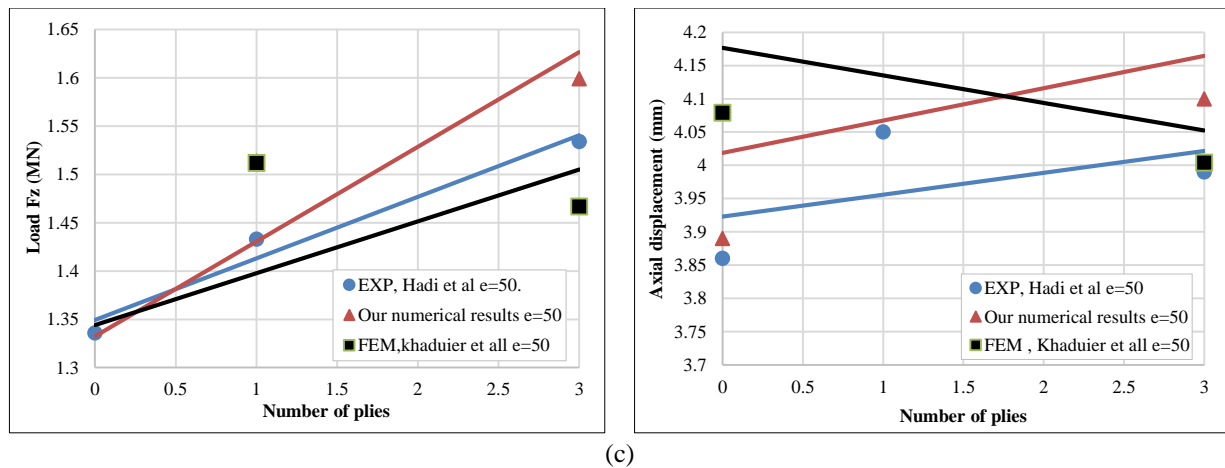

(a)

(b)

(c)

Figure 9. Load and Displacement versus number of CFRP plies for different eccentricity (a) e=0; (b) e=25; and (c) e=50

Our achieved results are in a good agreement with the experimental data released by Berthet et al. (2005) [29] as shown in Figure 7. In fact, this research team showed that for high strength concretes HSC with $\acute{f}_{co} > 50 MPa$, the value of the confinement efficiency coefficient k_1 decreases when the maximum compressive strength of the concrete $\acute{f}_{co}$ increases. Our numerical results show that the FEM code [25] that has been used in this analysis reproduces with high accuracy the experimental behavior of the confined concrete as a function of the confinement's level.

The current numerical FEM model is able to satisfactorily reproduce the damaging elastoplastic behavior of the concrete with a relative error ranging from 0.03 to 6%. In addition, the simulation's results demonstrate the capacity of the model to predict with accuracy the ultimate strength of the concrete and provide an appreciation of the correct ultimate displacement with regard to the engineering expectations.

The contours of the axial displacement are presented in Figure 10 for the three levels of the considered confinement and for the three types of the applied loading. The results are presented at the failure instant of the PRF composite. It was found that the maximal zone of the displacements is located on the upper surface of the column, while the minimal zone of the displacements is located on the lower embedded surface.
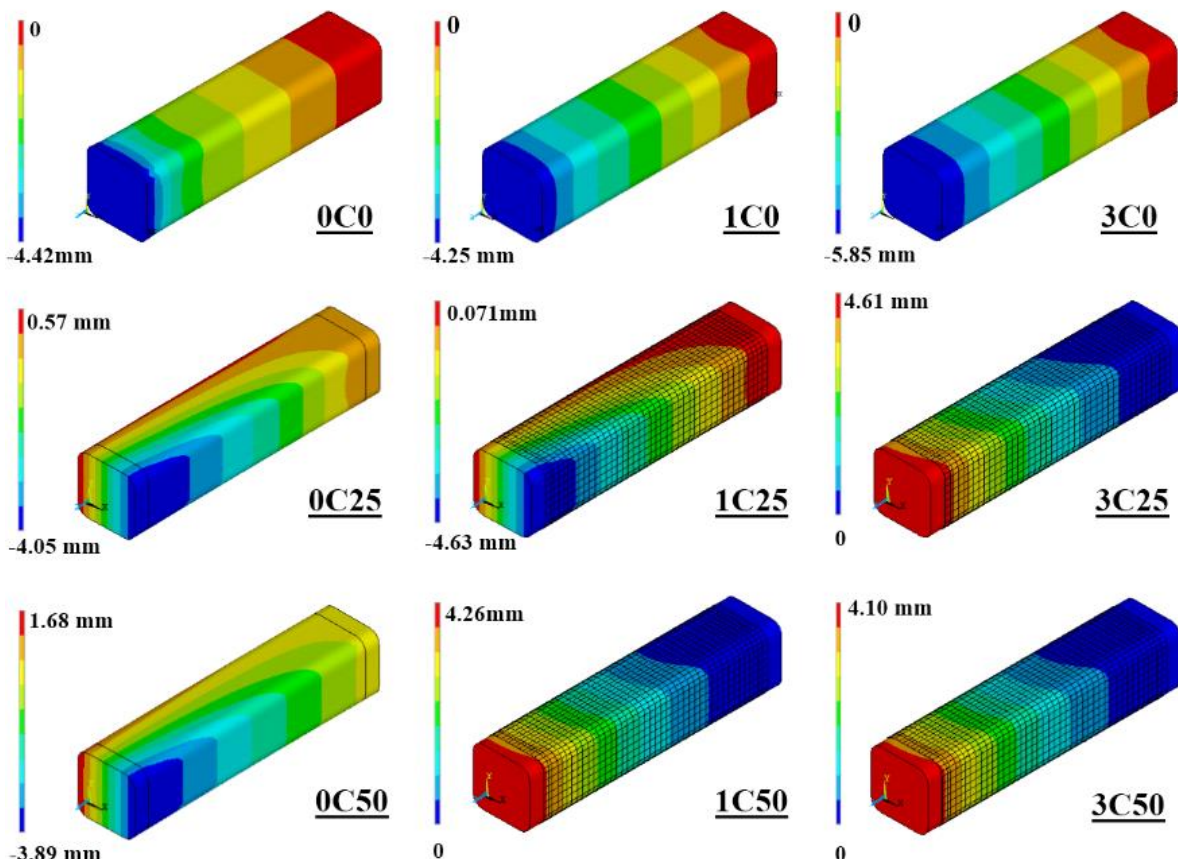

Figure 10. Contours displacement of confined and unconfined specimens under concentric and eccentric loading

The failure of the square specimens confined with CFRP was marked by the failure in the composite shell, which is located at the corners due to the stress concentration in these regions. Therefore, cracks are initiated in the corner zone and then are propagated to adjacent corners across the face of the specimen (Figure 11). The experimental and the numerical observed failure modes are principally the same. The criterion for the end of the analysis is the non-convergence of the solution, which is caused by the sudden failure of the CFRP jacket. Obviously, once the CFRP jacket fails, the concrete also fails in a very brittle way. At this stage, the steel bars and stirrups had yielded as shown in Figure 12 (f_y=561 MPa), and the stirrups touched their ultimate strain with largely column deformation. The criterion for the end of the numerical program is the non-convergence caused by the failure of fibers in the CFRP jacket.
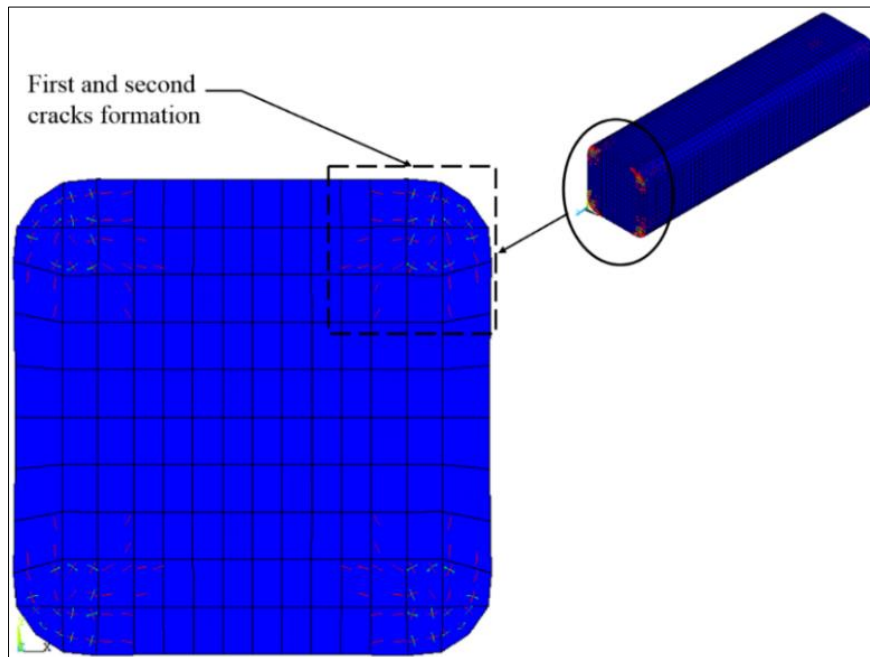

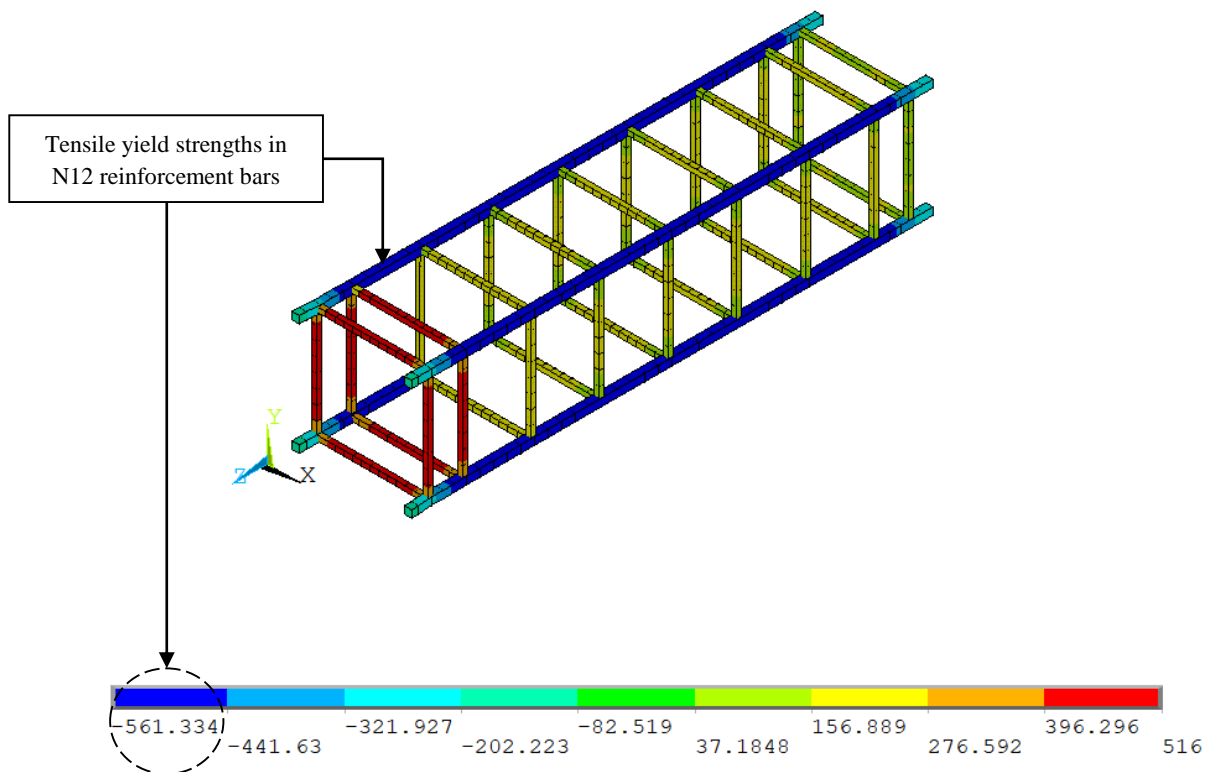**Figure 11. First and second cracks formation in the RC column**

Figure 12. Contours of X-stresses of steel reinforcement

4. Conclusions

The study presented in this paper was based on the structural performance of HSC columns confined by using a carbon fiber-reinforced polymer (CFRP) jacket. Both experimental and numerical comparisons were performed for RC specimens to investigate the influence of the materials properties, the loading eccentricity, and the number of CFRP layers on the columns' behavior and load carrying capacity. The most important outcomes derived from the performed simulations can be listed as follows:

- Compared to an unconfined column, CFRP wrapping clearly increased peak load capacities by 16.35% for the case of three applied plies. Moreover, no significant increase in maximum load was obtained when the columns were wrapped with one layer of CFRP jacket.

- The confined CFRP columns showed a higher gain in the ultimate axial displacement (33%) more than the load-carrying capacities (16.35%). Besides, the gain in strength and ductility decreases with the increase in concrete compressive strength.

- The CFRP wrapping had a significant effect on the maximum load of eccentrically loaded columns compared to concentrically loaded columns by increasing the compressive strength with a value of 15% gain compared to the unconfined column.

- The governing failure mode for the axially loaded column will in most cases be either crushing of the concrete or tensile failure of the CFRP fibers. The experimental and the numerical observed failure modes are principally the same.

- The current numerical FEM model is able to reproduce the damaging elastoplastic behavior of the concrete with good accuracy at all the stages of loading until failure.

- FRP is an excellent material that can be used to increase the load carrying capacity, the safety, and ductility of RC columns. However, additional experimental and numerical tests using different configurations of FRP materials and taking into account various grades of concrete and different geometries of columns are recommended before generalizing the findings of this study.

5. Declarations

5.1. Author Contributions

Conceptualization, M.Y.; methodology, M.Y. and S.F.; software, M.Y. and I.K.; validation, M.Y., S.F. and T.T.; writing—original draft preparation, M.Y., S.F. and I.K.; writing—review and editing, T.T. and I.K.; All authors have read and agreed to the published version of the manuscript.

5.2. Data Availability Statement

The data presented in this study are available in the.

5.3. Funding

The authors received no financial support for the research, authorship, and/or publication of this article.

5.4. Conflicts of Interest

The authors declare no conflict of interest.

6. References

[1] Shin, J., & Jeon, J. S. (2022). Seismic damage mitigation strategy using an FRP column jacketing system in gravity-designed reinforced concrete building frames. Composite Structures, 279. doi:10.1016/j.compstruct.2021.114700.

[2] Maheswaran, J., Chellapandian, M., & Arunachelam, N. (2022). Retrofitting of severely damaged reinforced concrete members using fiber reinforced polymers: A comprehensive review. Structures, 38, 1257–1276. doi:10.1016/j.istruc.2022.02.059.

[3] Salesa, A., Esteban, L. M., & Barris, C. (2022). Confinement of FRP concrete columns: Review of design guidelines and comparison with experimental results. Materiales de Construcción, 72(345), e274. doi:10.3989/mc.2022.03821.

[4] Saleh, E., Tarawneh, A., Almasabha, G., & Momani, Y. (2022). Slenderness limit of FRP-confined rectangular concrete columns. Structures, 38, 435–447. doi:10.1016/j.istruc.2022.02.030.

[5] Bedirhanoglu, I., Ilki, A., & Triantafillou, T. C. (2022). Seismic Behavior of Repaired and Externally FRP-Jacketed Short Columns Built with Extremely Low-Strength Concrete. Journal of Composites for Construction, 26(1), 4021068. doi:10.1061/(asce)cc.1943-5614.0001179.

[6] Al-Rousan, R. Z. (2022). Cyclic behavior of alkali-silica reaction-damaged reinforced concrete beam-column joints strengthened with FRP composites. Case Studies in Construction Materials, e00869. doi:10.1016/j.cscm.2022.e00869.

[7] Du, Y., Gao, D., Chen, Z., Zheng, Z., & Wang, X. (2022). Behaviors of FRP confined rectangular concrete-filled thin-walled steel tubular stub columns using high-strength materials under axial load. Composite Structures, 280, 114915. doi:10.1016/j.compstruct.2021.114915.

[8] Sanginabadi, K., Yazdani, A., Mostofinejad, D., & Czaderski, C. (2022). RC members externally strengthened with FRP composites by grooving methods including EBROG and EBRIG: A state-of-the-art review. Construction and Building Materials, 324, 126662. doi:10.1016/j.conbuildmat.2022.126662.

[9] Bai, Y. L., Zhang, Y. F., Jia, J. F., Mei, S. J., Han, Q., & Dai, J. G. (2022). Simplified plasticity damage model for large rupture strain (LRS) FRP-confined concrete. Composite Structures, 280, 114916. doi:10.1016/j.compstruct.2021.114916.

[10] Zeng, J. J., Zhu, D. H., Liao, J. J., Zhuge, Y., Bai, Y. L., & Zhang, L. (2022). Large-rupture-strain (LRS) FRP-confined concrete in square stub columns: Effects of specimen size and assessments of existing models. Construction and Building Materials, 326, 126869. doi:10.1016/j.conbuildmat.2022.126869.

[11] Ye, Y. Y., Zeng, J. J., & Li, P. L. (2022). A State-of-the-Art Review of FRP-Confined Steel-Reinforced Concrete (FCSRC) Structural Members. Polymers, 14(4), 677. doi:10.3390/polym14040677.

[12] Fukuyama, H., & Sugano, S. (2000). Japanese seismic rehabilitation of concrete buildings after the Hyogoken-Nanbu earthquake. Cement and Concrete Composites, 22(1), 59–79. doi:10.1016/S0958-9465(99)00042-6.

[13] Wu, H.-C., & Eamon, C. D. (2017). Introduction. In Strengthening of Concrete Structures using Fiber Reinforced Polymers (FRP) (pp. 1–10). doi:10.1016/b978-0-08-100636-8.00001-6.

[14] Beroual, S., & Samai, M. L. (2021). Determination of Reinforced Concrete Rectangular Sections Having Plastic Moments Equal to all IPE Profiles. Civil Engineering Journal, 7(4), 614–632. doi:10.28991/cej-2021-03091677.

[15] Opabola, E. A., Elwood, K. J., & Liel, A. B. (2021). Evaluation of seismic performance of as-built and retrofitted reinforced concrete frame structures with LAP splice deficiencies. Earthquake Engineering and Structural Dynamics, 50(12), 3138–3159. doi:10.1002/eqe.3503.

[16] de Diego, A., Arteaga, Á., & Fernández, J. (2019). Strengthening of square concrete columns with composite materials. Investigation on the FRP jacket ultimate strain. Composites Part B: Engineering, 162, 454–460. doi:10.1016/j.compositesb.2019.01.017.

[17] Fanaradelli, T., Rousakis, T., & Karabinis, A. (2019). Reinforced concrete columns of square and rectangular section, confined with FRP – Prediction of stress and strain at failure. Composites Part B: Engineering, 174, 107046. doi:10.1016/j.compositesb.2019.107046.

[18] Hasan, H. A., Sheikh, M. N., & Hadi, M. N. S. (2019). Maximum axial load carrying capacity of Fibre Reinforced-Polymer (FRP) bar reinforced concrete columns under axial compression. Structures, 19, 227–233. doi:10.1016/j.istruc.2018.12.012.

[19] Abdulla, M. D., & Khaduier, Z. A. (2018). Nonlinear Finite Elements Analysis of Reinforced Concrete Columns Strengthened With Carbon Fiber Reinforced Polymer (CFRP). Journal of University of Babylon for Engineering Sciences, 26(3), 75–97. doi:10.29196/jub.v26i3.618.

[20] Al-Rousan, R. (2020). Behavior of Circular Reinforced Concrete Columns Confined with CFRP Composites. In Procedia Manufacturing, 44, 623–630. doi:10.1016/j.promfg.2020.02.247.

[21] Hawileh, R. A., Musto, H. A., Abdalla, J. A., & Naser, M. Z. (2019). Finite element modeling of reinforced concrete beams externally strengthened in flexure with side-bonded FRP laminates. Composites Part B: Engineering, 173, 106952. doi:10.1016/j.compositesb.2019.106952.

[22] Al-Nimry, H., & Neqresh, M. (2019). Confinement effects of unidirectional CFRP sheets on axial and bending capacities of square RC columns. Engineering Structures, 196, 109329. doi:10.1016/j.engstruct.2019.109329.

[23] Mhanna, H. H., Hawileh, R. A., & Abdalla, J. A. (2019). Shear strengthening of reinforced concrete beams using CFRP wraps. Procedia Structural Integrity, 17, 214–221. doi:10.1016/j.prostr.2019.08.029.

[24] Hadi, M. N. S., & Widiarsa, I. B. R. (2012). Axial and Flexural Performance of Square RC Columns Wrapped with CFRP under Eccentric Loading. Journal of Composites for Construction, 16(6), 640–649. doi:10.1061/(asce)cc.1943-5614.0000301.

[25] ANSYS. (2017). ANSYS Help. Release 18.20. Available online: https://www.ansys.com/it-solutions/platform-support/previous-releases (accessed on January 2022).

[26] Wight, J. K., & MagGregor, J. G. (2011). Reinforced Concrete: Mechanics and Design (6th Ed.). Prentice Hall, Hoboken, United States.

[27] Lam, L., & Teng, J. G. (2003). Design-oriented stress-strain model for FRP-confined concrete in rectangular columns. Journal of Reinforced Plastics and Composites, 22(13), 1149–1186. doi:10.1177/0731684403035429.

[28] Teng, J. G., Chen, J. F., Smith, S. T., & Lam, L. (2003). Behaviour and strength of FRP-strengthened RC structures: A state-of-the-art review. Proceedings of the Institution of Civil Engineers: Structures and Buildings, 156(1), 51–62. doi:10.1680/stbu.2003.156.1.51.

[29] Berthet, J. F., Ferrier, E., & Hamelin, P. (2005). Compressive behavior of concrete externally confined by composite jackets. Part A: Experimental study. Construction and Building Materials, 19(3), 223–232. doi:10.1016/j.conbuildmat.2004.05.012.